A small-angle neutron scattering study on poly(ethylene oxide) crystals

Geoffrey Allen
Department of Chemical Engineering and Chemical Technology, Imperial College, London SW7 2BY, UK

and Takeshi Tanaka
Institute for Chemical Research, Kyoto University, Uji, Kyoto 611, Japan
(Received 12 October 1977)

Small-angle neutron scattering measurements were made on poly(ethylene oxide) (PEO) crystallized from the melt. Samples with the deuterated species (DPEO) as a matrix present distinct Bragg peaks from which the lamella spacings can be determined. As a result of strong void-scattering, quantitative analysis of the low-angle regime of these scattering curves is not possible. Samples with the protonous species as a matrix, for which void-scattering is expected to be negligibly small, present unusual scattering curves indicating that they consist of two components, i.e. the intramolecular and intermolecular interference terms. A quantitative analysis of these curves indicates: (1) the solute DPEO molecules are embedded in the crystalline structure of the matrix, assuming rod-like conformations but (2) forming essentially homogeneous aggregates of a few to tens of the DPEO molecules, depending on the crystallization temperature and the DPEO concentration; (3) the DPEO molecules or aggregates are distributed in space in a non-random manner that corresponds to the presence of inhomogeneous 'domains' having root-mean-square radii of about 250 Å, and each containing about 100 DPEO molecules.

INTRODUCTION

Small-angle neutron scattering (SANS) is proving to be a particularly valuable method for studying the conformational behaviour of polymer molecules in glasses, rubbers and solutions covering a wide range of concentrations. For example, it has been shown that amorphous polymers in the bulk such as poly(methyl methacrylate)[1], polystyrene[2] and molten poly(ethylene oxide)[3] assume conformations indistinguishable from those in θ-solvents. More recently the conformational behaviour of polymer chains in solutions of intermediate and high concentration have been established with respect to concentration and temperature[4–6]. In all such studies, random orientation of the chains is assumed with respect to other chains and to the incident beam, and so the data are analysed in terms of the familiar scattering law $S(Q)$ valid at low concentration C and small values of Q:

$$KC/S(Q) = [MP(Q)]^{-1} + 2A_2C \quad (1)$$

$$P(Q) = 1 + R_G^2Q^2/3 \quad (2)$$

$$Q = (4\pi/\lambda)\sin(\theta/2)$$

K is a constant, θ is the scattering angle, λ is the wavelength, M and R_G are the molecular weight and the root-mean-square radius of gyration of the solute molecule, respectively, and A_2 is the second virial coefficient.

Measurements on crystalline polymers have proved to be more difficult to interpret. For example, Schelten *et al.*[7] reported that unless a dispersion of deuterated polyethylene in protonous polyethylene is carefully prepared, the deuterated species forms molecular clusters both above and below the melting temperature. There is considerable disagreement on the interpretation of the scattering curves obtained from crystallized polyethylene samples[7,8]. Apart from the fact that in the crystal molecules are highly oriented and thus strongly correlated, the parameters A_2 and R_G are now much less clearly defined when the results are analysed in this simple way. Complications may arise from the fact that all polymer crystals are essentially two-phase structures containing both crystalline and amorphous regions. (Even for an amorphous, fully protonated two-phase system obtained with an AB block copolymer of styrene–butadiene, a huge Bragg peak can be observed which arises from the slight contrast between styrene and butadiene domains[9].)

We have made SANS measurements on poly(ethylene oxide) (PEO) crystals in an attempt to obtain information on the conformation of individual molecules. The polymer is available with narrow molecular weight distribution in a molecular weight range of 200–10 000. It is well known that when crystallized from the melt, this polymer forms large spherulites each consisting of a large number of lamellae. The molecules are folded normal to the lamella surface, and the number of folds per molecule can be selectively controlled by the crystallization temperature. The molecular axes are normal to the radii of the spherulite, and therefore the probability of finding a molecule oriented in a given direction is uniformly independent of direction. Thus the data can be analysed, in principle, by assuming that equations (1) and (2) are valid. Finally, the system is interesting because the difference between the force fields of protonous

Table 1 Samples of poly(ethylene oxide) and crystalline structure of the matrices[a]

	Solute		Matrix			
Sample	Molecular weight	Concentration (%)	Molecular weight	f	d(Å)	T_c (°C)
1	3000 H	3.18	6000 D	1	170	40
2	6000 H	3.18	6000 D	1	170	50
3	10000 H	3.18	6000 D	1	170	55
				0	330	
4	10000 H	3.18	6000 D	1	170	40
5	EG H	3.18	6000 D	1	190	50
6	6000 D	2.92	3000 H	0	200	50
8	6000 D	1.64	6000 H	1	200	50
9	6000 D	3.02	6000 H	1	200	50
10	6000 D	4.54	6000 H	1	200	50
11	6000 D	3.17	6000 H	0	400	56
				1	200	
12	6000 D	3.13	10000 H	1	400	57
13	6000 D	2.38	10000 H	2	270	50
14	6000 D	3.22	10000 H	3	200	40

[a] Abbreviations and notes: f and d are fold number and lamella spacing, respectively, both estimated from the published data[10] except for those of samples 1–5 which were determined by the present SANS measurements; T_c is the crystallization temperature; EG is ethylene glycol; and H and D denote the protonous and deutrated species, respectively

and the deuterated species which may contribute to the clustering observed in polyethylene dispersions should be less marked in PEO dispersions because of the lower hydrogen content in PEO.

EXPERIMENTAL

Materials

Deuterated poly(ethylene oxide) (DPEO) was prepared by using fully deuterated ethylene oxide as the monomer and the disodium salt of protonous ethylene glycol as the initiator. The molecular weight M_n and the molecular weight ratio M_w/M_n were found to be 6000 and 1.15, respectively, by g.p.c. analysis. The protonous poly(ethylene oxides) (HPEO) with M_n = 3000, 6000 and 10 000 were obtained commercially; the M_w/M_n ratios were all within 1.0 to 1.2.

Solid samples with controlled thickness of about 1.5 mm were prepared by melting the mixture of DPEO and HPEO at about 85°C, stirring the melt mechanically and allowing the solution to crystallize on a temperature-controlled plate. To ensure intermixing of D- and HPEO, a few samples were also made from the mixture which was first dissolved in a solvent (benzene, 60°C) and freeze-dried from the solution. (It was found that the pretreatment resulted in no detectable difference in the results of SANS measurements.) The samples prepared are listed in *Table 1* together with structural parameters such as lamella spacing d and number of folds f quoted from the literature[10].

Neutron scattering

Measurements were made using the low-angle diffractometer D11 at the High Flux Beam Reactor at ILL, Grenoble[11]. Wavelengths of 10.0 and 9.85 Å were used together with a sample-to-detector distance of 5.365 m.

RESULTS

Scattering from HPEO and DPEO backgrounds

In order to obtain the required information it is necessary that the contrast factor, $(b_D - b_H)^2$, where b_D and b_H are the scattering lengths of the deuterated and proton monomer units, respectively, should be large enough and, in addition, that the influence of voids or impurities should be small. *Figure 1* shows some spectra obtained.

Curve A in the Figure is for a DPEO background. Extremely strong scattering can be seen at low angles, which amounts to several thousand counts at the lowest angle accessible. At a high angle, corresponding to $Q \sim 3 \times 10^{-2}$ Å^{-1}, there is a distinct peak which corresponds to a lamella spacing of d = 190 Å. This is a half of the value to be expected when the molecule is fully extended[10,12] indicating that the molecules are folded once. This Bragg peak arises from the density difference between the crystalline and amorphous regions. Voids or impurities, especially moisture and, for the present sample, the protonous chain ends, will also enhance the contrast, because they will concentrate in the amorphous region.

It is interesting to note that if we add 3% of H ethylene glycol to this sample, the peak height becomes about 15 times larger (curve D, *Figure 1*), while the intensity at low angles remains almost the same. Clearly, the added monomer goes into the amorphous region, enhancing the contrast. Since the low-angle scattering does not change, the monomer is essentially, molecularly dispersed.

We deduce that the strong scattering at low angles is predominantly due to large voids. This also means that the samples with DPEO matrices are not suitable for the present purpose.

On the other hand, the scattering from an HPEO background is small and uniform for all angles, and no influence of voids is observed (curve B, *Figure 1*). Thus, we assume that the 'scattering length' b_V of voids is very close to that of HPEO, i.e., $b_V \sim b_H$. This allows the estimation of the contribution of void-scattering for a sample containing a volume fraction Φ_D of DPEO molecules; void-scattering $\propto \Phi_D^2(1 - \Phi_V)^2(b_D - b_H)^2$. Here Φ_V is the volume fraction of voids. Since in our experiments Φ_V will be of the same order for any sample, we may consider that the void-scattering is proportional to Φ_D^2. For the present samples

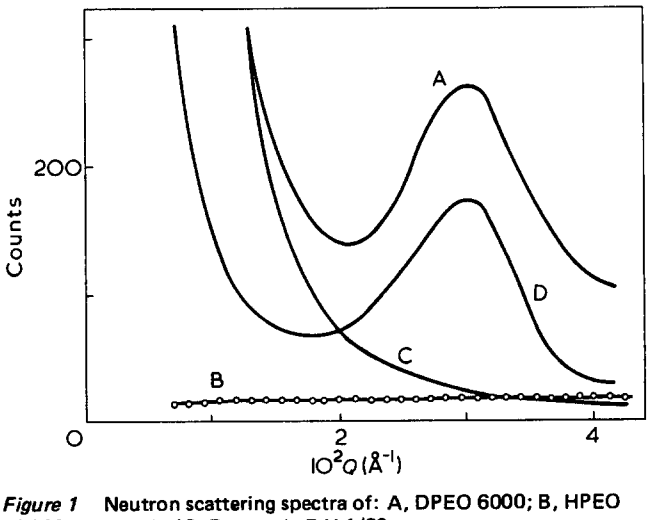

Figure 1 Neutron scattering spectra of: A, DPEO 6000; B, HPEO 10000; C, sample 12; D, sample 5 X 1/20

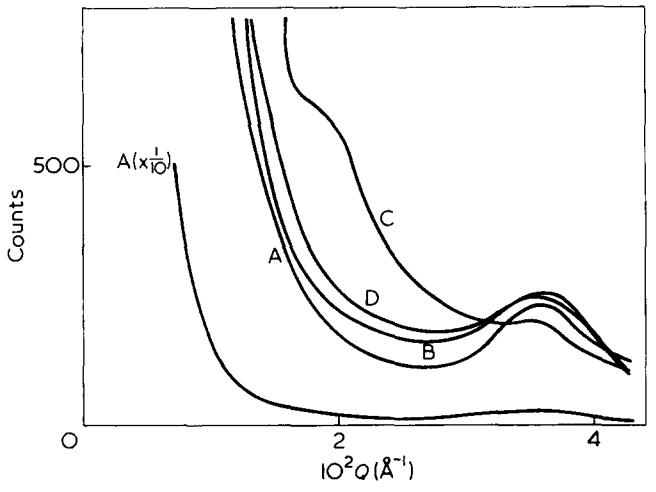

Figure 2 Neutron scattering spectra of samples with DPEO 6000 as the matrix. A, sample 1; B, sample 2; C, sample 3; D, sample 4

containing a few percent of DPEO, the void-scattering should be of the order of a few counts even at the lowest angle accessible (under the same sample condition and the same count levels). This is small enough to be neglected, since we observed several hundred counts at low angles for those samples (cf. curve C, *Figure 1*). However, the void-scattering will pose a serious problem when the sample counts are smaller.

Scattering from HPEO in DPEO matrix

As shown above, samples which have DPEO as a matrix give Bragg peaks at high angles. Some examples are shown in *Figure 2*. These samples contain 3.18% of HPEO of different molecular weight and/or were crystallized at different temperature. The lamella spacing corresponding to the observed peak is in reasonable agreement with the value expected from the crystallization conditions. For example, sample 3 (curve C, *Figure 2*) which was crystallized at 55°C gives two peaks indicating the presence of two kinds of lamellae, one with the molecules extended and the other with them folded once. This agrees with the X-ray measurements[10]. However, the peak positions appear to shift to angles somewhat larger than those observed for pure DPEO (compare *Figure 2* with curve A of *Figure 1*). The reason for this is not clear, since it is rather hard to believe that such a small amount of HPEO can alter the crystalline structure significantly.

On the other hand, the height of the peak does not seem to be changed by addition of HPEO. This could suggest that the added molecules of HPEO are more evenly distributed between crystalline and amorphous regions than is the case with the corresponding wt fraction of H-ethylene glycol. It has been pointed out that during the course of crystallization some fractionation occurs between molecules with different length[13], and the shorter chains tend to be fractionated out into the amorphous region[10]. This effect has been most clearly observed when the shorter chains are monomers. However, so far as the present samples are concerned, i.e. the molecular weight ratio of HPEO to DPEO ranges from 0.5 to 1.7, the fractionation phenomenon is not detectable.

The low-angle part of the spectra, on the other hand, depends on both molecular weight of the solute HPEO and the crystallization temperature. The higher the molecular weight and the higher the crystallization temperature, the stronger scattering is observed at low angles. The effect of molecular weight is self-explanatory, since larger particles scatter more strongly. The effect of crystallization temperature would be most simply explained by the aggregation of the solute HPEO molecules. This point will become clearer in the following section. Further analysis on the low-angle part of the spectra was not possible for the reason described in the previous section.

Scattering from DPEO in HPEO matrices

Because of the low scattering from voids, this series of samples is more suitable for the investigation of conformational properties of PEO molecules. Some results are presented in *Figures 3* and *4*. The scattering curve for the melt is normal, but for the solid samples plots of $C_D/S(Q)$ vs. Q^2 have a pronounced sigmoid shape. For this reason we present plots of $[C_D/S(Q)]^{1/2}$ vs. Q^2, because this plot is more readily extrapolated to zero value of Q to provide an intercept on the ordinate. Here C_D is the weight fraction of DPEO. The scale of the ordinate is chosen to give unity at zero angle for the reference sample run in the melt (curve A, *Figure 3*). The background has been subtracted, and a correction applied for density difference. Thus, the intercept should be proportional to the reciprocal of $M_w^{1/2}$ for a simple system, e.g. the melt, if we assume that the DPEO molecules are molecularly dispersed in a statistical manner so that $A_2 = 0$. In our results, the radius of gyration of DPEO estimated from the melt is 35 Å, which fits the known M_w vs. R_G relationship[3].

The scattering curves for the solid samples are abnormal in two respects. One is that each curve consists of two components; one branch at low Q of large slope and the other at high Q of smaller slope. The other is that the intercepts obtained by extrapolating either the linear high-Q branches or the low-Q branches correspond to values of M_{app} (defined at the concentration used) which are much larger than the value of M for the melt sample. Such two-branch plots are sometimes observed in light scattering studies. They are usually caused by dust or microgel, and the extrapolation from the high-Q regime usually gives a reasonable value of M_{app}. In our case, voids or dust cannot be the cause of the anomalous scattering, as pointed out above. Hence, we have

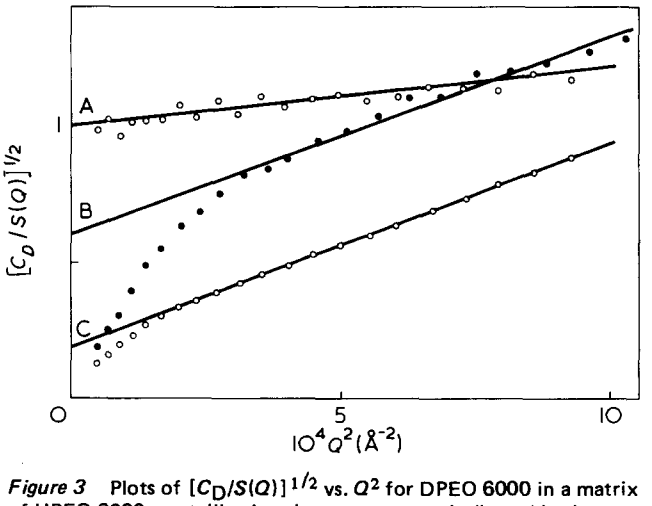

Figure 3 Plots of $[C_D/S(Q)]^{1/2}$ vs. Q^2 for DPEO 6000 in a matrix of HPEO 6000 crystallized at the temperatures indicated in the Figure. The ordinate scale was normalized to unity for the reference sample run in the melt (72°C) (curve A); B, T_c = 50°C; C, T_c = 56°C

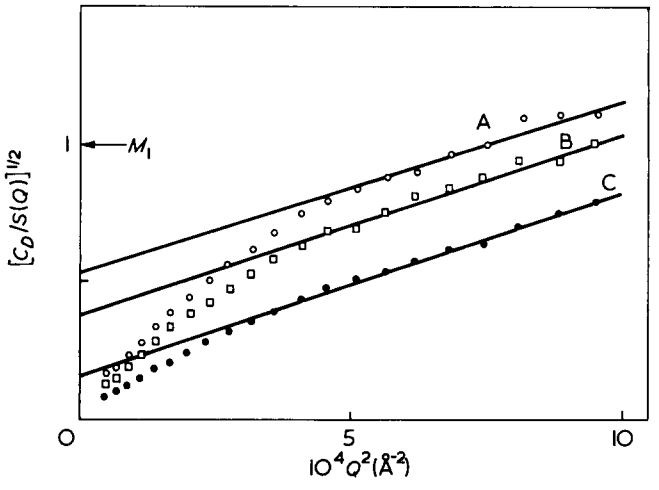

Figure 4 Plots of $[C_D/S(Q)]^{1/2}$ vs. Q^2 for DPEO 6000 in a matrix of HPEO 10000 crystallized at the temperatures indicated in the Figure. The ordinate scale was normalized to unity for the reference sample run in the melt (see *Figure 3*). A, T_c = 40°C; B, T_c = 50°C; C, T_c = 57°C

to conclude that the anomalous scattering comes from the solute DPEO molecules themselves, which are by no means randomly (statistically) dispersed in the HPEO matrix.

One may argue that even though the DPEO molecules may be randomly dispersed, there might be effects of intermolecular interference arising from the fact that they are embedded with radial correlation in the lamella structure, and the molecular centres are bound on the parallel planes normal to molecular axes, each passing through the centre of a lamella. However, this does not appear to be the cause of the anomalous scattering, since the probability of a pair of segments (each belonging to different DPEO or HPEO molecules) being a distance R apart should be uniform for all values of R hence giving no effects of intermolecular interference, in the assumption that the DPEO and HPEO molecules are thermodynamically identical. Of course, scattering can still arise from the density difference between the amorphous and crystalline regions. However, as pointed out previously, this scattering must be very small. In fact, we have detected no Bragg peak for any sample of this series (cf. curve C, *Figure 1*).

Moreover, the above hypothesis is strongly rejected by the fact that when compared with the other fixed conditions, the scattering intensity systematically becomes stronger as the crystallization temperature T_c becomes closer to the melting temperature T_m (about 59°C). For example, the value of M_{app} for sample 11 (T_c = 56°C) obtained by extrapolating the high-Q branch of the curve is nearly 15 times as large as that for sample 9 (T_c = 50°C). It would be quite difficult to explain such a drastic change in scattering intensity in terms of the *a priori* difference in structure expected for the two samples.

For these reasons, we conclude that some form of aggregation of DPEO molecules occurs during the course of crystallization. This seems to explain the strong T_c-dependence of scattering intensity most simply, since the 'segregation' between D- and H-species, if any occurs, must be a sensitive function of the super-cooling temperature $\Delta T = T_m - T_c$. When ΔT is large crystallization occurs in a short time with the random dispersion of the solute molecules achieved in the melt essentially being frozen. When ΔT is small, the segregation should occur most critically resulting in large aggregates of the solute molecules. This is in line with our observations (cf. *Figures 3* and *4*).

There is little possibility that due to the incompatibility of the two species, one species is fractionated out into the amorphous since, if so, a contrast will be produced between the amorphous and crystalline regions, and we should have observed a marked Bragg peak as is seen, for example, when the protonous monomer is added to the DPEO matrix.

DISCUSSION

Then, of what form are the aggregates? A clue should lie in the shape of the scattering curves.

If we assume any particular shape for the DPEO aggregates such as a disc, rod, cylinder, sphere or ellipsoid, and assume further that HPEO is excluded from the aggregates, the computed scattering envelope fails to explain the shape of the curves over the observed range of Q. In addition, the apparent radii of gyration estimated from the initial slopes (i.e. the low-Q branches) of the observed scattering envelopes are too large to correspond to any imaginable rigid particle consisting of such a small number of molecules which corresponds to the intercept on the ordinate.

Instead, we can assume that there exist 'domains' of relatively large size in which the DPEO molecules have a higher than average population. That is to say, we are observing the domains at low Q, and at high Q the individual particles (which may not necessarily consist of a single molecule, as will be seen later).

More generally, a heterogeneous system is characterized in terms of the pair distribution function $p(r)$, which is the probability density of finding the centre of mass of any other molecule a distance r apart from that of a given molecule. If we define $g(r) = p(r) - p_0$, where p_0 is the average probability (i.e. the number density of solute molecules averaged over the whole system), and assume that $g(r)$ is spherically symmetric (as pointed out previously, this should not be the case for our system, but if the inhomogeneity extends over a large enough region, we may assume this as a first approximation). Then the following scattering law can be derived for our system since it will have parallel correlation of molecular axes over the spacial region of practical importance:

$$S(Q)/KC_D = MP(Q)[1 + AG(Q)] \quad (3)$$

$$G(Q) = \int g(r)\exp(iQr)dr / \int g(r)dr \quad (4)$$

$$A = \int g(r)dr \quad (5)$$

For a system with repulsive interactions between solute molecules (i.e. excluded volume effects), $p(r) < p_0$ or $g(r) < 0$ for a certain range of r. Then writing $g(r) = -p_0[1 - p'(r)]$ with $p'(r) = p(r)/p_0$, we see that equations (3)–(5) are identical with the Zernicke–Prins equation[14], and further with equation (1) by assuming that $G(Q) = P(Q)$. For our present system, a typical shape of $g(r)$ must be such that $g(r) > 0$ for small r and decreases with increase of r to approach zero for sufficiently large r.

Now expanding the right hand side of equation (4), we have:

$$G(Q) = 1 - (1/6)\langle r^2\rangle Q^2 + \ldots \quad (6)$$

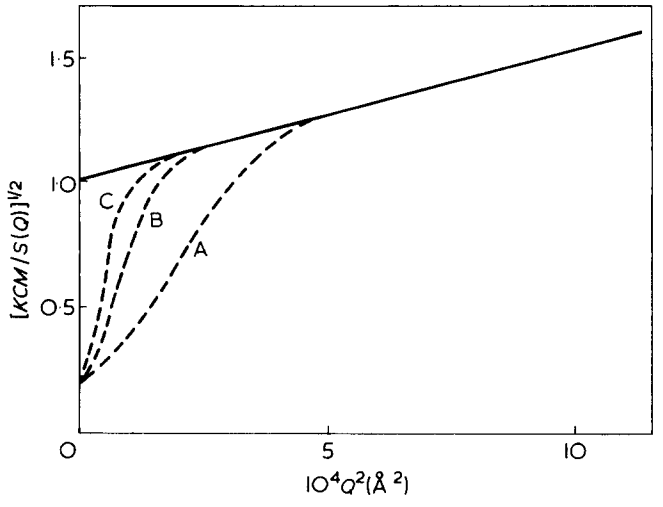

Figure 5 Calculated scattering curves for an inhomogeneous system with $N = 25$ and $r_G = 200$ (A); 300 (B); 400 Å (C). The $G(Q)$ function was assumed to be Gaussian, i.e. $G(Q) = \exp(-r_G^2Q^2/3)$, and the $P(Q)$ function (——) was calculated for a rod of length 200 Å ($R_G = 58$ Å). It was noted that for this hypothetical system the values of M_{app} and R_{app} estimated by linearly extrapolating a high-Q branch of the curve (say, $5 \times 10^{-4} < Q < 10 \times 10^{-4}$) are smaller by about 5 and 15% than the true values of M and R_G, respectively, if $r_G > 200$ Å

$$\langle r^2\rangle = \int_0^\infty 4\pi r^4 g(r)\mathrm{d}r \Big/ \int_0^\infty 4\pi r^2 g(r)\mathrm{d}r \qquad (7)$$

The parameter $\langle r^2\rangle$ quantitatively describes the extent of inhomogeneity. A more comprehensive parameter may be r_G^2, the mean-square radius of gyration of the equivalent 'domain', which is given by:

$$r_G^2 = (1/2)\langle r^2\rangle \qquad (8)$$

By a similar argument, the parameter A given by equation (5) is equal to $N-1$, where N is the number of particles in a 'domain'.

Figure 5 shows the results of some model calculations for an inhomogeneous system in which domains are randomly dispersed in the system, and in each domain $N = 25$ rod-like particles of length 200 Å are dispersed randomly with respect to the centres of mass of the particles but in parallel to each other. The domain scattering $G(Q)$ was approximated by a Gaussian function $\exp[-(1/3)r_G^2Q^2]$, which fits those of most three-dimensional uniform-density bodies over a wide range of Q. The Figure shows that the $[KC/S(Q)]^{1/2}$ vs. Q^2 plots clearly split into the two components. When r_G is large enough, say $r_G > 200$ Å, the low-Q component rapidly becomes less important with increase in Q, indicating that the extrapolation of the high-Q branch will give not-so-unreasonable estimates of M and r_G.

Table 2 summarizes the results of the analysis based on equations (3)–(8) for the data obtained above. Here v_{app} is the apparent molecular weight relative to that estimated for the melt, and R_{app} is the apparent root-mean-square radius of a particle. Both v_{app} and R_{app} are estimated from the high-Q branches of the scattering curves. The values of r_G and N were obtained from the plots of $\ln[S(Q)/KC_DMP(Q) - 1]$ vs. Q^2, as indicated above.

In the Table, we notice that the values of v_{app} are often much larger than unity, indicating that the 'particles' do not consist of a single molecule. We see that they systematically change with the crystallization condition: when the matrix molecular weight M_H and C_D are the same, there is a very strong dependence of v_{app} on T_c, i.e. v_{app} increases with increasing T_c, and when M_H and T_c are the same, v_{app} increases slightly with increasing C_D. So far as samples 8–10 are concerned, v_{app} appears to become unity at zero concentration. The molecular weight difference between DPEO and HPEO does not seem to have any apparent effects on v_{app}.

The values of R_{app} are also much larger than those estimated for the melt. In this connection, it may be worth noting that aggregates formed in solution or the amorphous melt, have relatively small values of R_{app} in spite of their large v_{app} values. For example, it has been reported[7] that for a polyethylene sample run in the melt v_{app} is estimated to be 10, but R_{app} is only 50%, slightly larger than the value for the sample with $v_{app} = 1$. One of our samples, 13, which has $v_{app} = 7$ presents a value of R_{app} nearly three times as large as that for the melt. This would suggest that the DPEO molecules are embedded in the crystalline structure of the matrix, assuming a rod-like conformation. A rod-like PEO molecule with $M = 6000$ has a radius of about 110Å when unfolded and of about 55 Å when folded once. The radii of aggregates consisting of tens of the rod-like molecules remain almost the same as that of a single molecule, in so far as the aggregates are in the form of a rigid bundle about a lamella long spacing. In view of the number of folds expected for the present samples (see *Table 1*), there seems to be a close correlation between the trends in the observed R_{app} and the calculated radii, even though the observed values are sometimes considerably larger than the calculated values.

However it should be borne in mind that the values of R_{app} as well as v_{app} can be in considerable error, partly because the extrapolation was made from a region of Q somewhat too high, and partly because we may not have succeeded in separating perfectly the $P(Q)$ and $G(Q)$ components. The latter point is especially relevant for those samples which present relatively large values of R_{app} compared with the values of r_G.

The estimated values of r_G are roughly the same for all the samples, i.e. $r_G = 250 \pm 30$ Å, independent of sample conditions such as T_c, C_D and M_H.

The estimated values of N are of the order of 10, and also are not seriously influenced by the sample conditions. These values of N correspond to the numbers of molecules per 'domain' (i.e. Nv_{app}) of the order of 100.

Table 2 Analysis of the scattering curves for DPEO 6000 in HPEO matrices[a]

Sample	Molecular weight of HPEO	C_D (%)	T_c (°C)	v_{app}	R_{app} (Å)	r_G (Å)	N
11 (melt)	6000	3.17	72	1	35		
6	3000	2.92	50	1.7	60	270	30
8	6000	1.64	50	1.4	65	260	35
9	6000	3.02	50	1.9	70	280	60
10	6000	4.54	50	2.3	70	280	60
11	6000	3.17	56	30	150	260	6
12	10000	3.13	57	40	160	220	9
13	10000	2.38	50	7.0	100	240	25
14	10000	3.22	40	3.5	80	220	25

[a] For the symbols, see *Table 1* and the text

From this analysis we have the following picture of the DPEO molecules dispersed in the HPEO matrices: the DPEO molecules are embedded in the crystalline structure of the matrices, assuming rod-like conformations and forming essentially homogeneous aggregates of a few to tens of molecules, depending on T_c and C_D. Irrespective of the sample conditions, strong scattering is observed at low Q arising from a non-random dispersion of the DPEO molecules or aggregates, which corresponds to the presence of inhomogeneous 'domains' of radius $r_G \sim 250$ Å, each containing about 100 DPEO molecules.

It is unlikely that the anomalous scattering shown by the present system comes from something related to the crystalline structure of PEO itself. Presumably, a small thermodynamical difference between the H- and D-species is responsible. The slight difference between their molecular force fields[15] could be the direct cause of the clustering of DPEO into rigid aggregates[7]. However, it is rather hard to believe that the difference in molecular force field alone can produce the inhomogeneity on such a large scale. A very small difference in melting temperature or crystallization rate may well mean that one species crystallizes faster than the other. If so, crystalline fragments formed at different stages of crystallization can be different in composition, thus giving inhomogeneous domains of large size. Clearly, more work is needed before this point could be established.

ACKNOWLEDGEMENTS

Thanks are due to Dr R. H. Mobbs for preparing the DPEO sample, and to Dr J. S. Higgins and Dr A. Maconnachie for aid in the SANS measurements. This work was supported by the Science Research Council.

REFERENCES

1 Kirste, R. G., Kruse, W. A. and Schelten, J. *Makromol. Chem.* 1973, **162**, 299
2 Cotton, J. P., Decker, D., Benoit, H., Farnoux, B., Higgins, J., Jannink, G., Ober, R., Picot, C. and des Cloizeaux, J. *Macromolecules* 1974, **7**, 863
3 Allen, G. *Proc. Roy. Soc. (A)* 1976, **351**, 381
4 Daoud, M., Cotton, J. P., Farnoux, B., Jannink, G., Sarma, G., Benoit, H., Duplessix, C., Picot, C. and de Gennes, P. G. *Macromolecules* 1975, **8**, 804
5 Cotton, J. P., Nierlich, M., Boue, F., Daoud, M., Farnoux, B., Jannink, G., Dupessix, R. and Picot, C. *J. Chem. Phys.* 1976, **65**, 1101
6 Richards, R. W., Maconnachie, A. and Allen, G. *Polymer* 1978, **19**, 266
7 Schelten, J., Wignal, G. D. and Ballard, D. G. H. *Polymer* 1974, **15**, 682
8 King, J. S., Summerfield, G. C., Higgins, J. S. and Ullman, R. reported in Strasbourg, 1975
9 Tanaka, T. and Allen, G. unpublished results
10 Arlie, J. P., Spegt, P. A. and Skoulios, A. E. *Makromol. Chem.* 1960, **99**, 160; 1967, **104**, 212; Gilg. and Skoulios, A. E. *Makromol. Chem.* **140**, 149
11 Schmatz, W., Springer, T., Schelten, J. and Ibel, K. *J. Appl. Crystallogr.* 1974, **7**, 96
12 Takahashi, Y. and Tadokoro, H. *Macromolecules* 1972, **6**, 672
13 Anderson, P. R. *J. Appl. Phys.* 1964, **35**, 67
14 Zernicke, F. and Prins, J. A. *Z. Phys.* 1927, **41**, 184
15 Stehling, F. S., Ergos, E. and Mandelkern, L. *Macromolecules* 1971, **4**, 672